ELSEVIER

Infrared Physics & Technology 41 (2000) 1–9

INFRARED PHYSICS & TECHNOLOGY

www.elsevier.com/locate/infrared

# Responsivity of infrared antenna-coupled microbolometers for air-side and substrate-side illumination

Javier Alda [1], Christophe Fumeaux [*], Michael A. Gritz, David Spencer [2], Glenn D. Boreman

*School of Optics / CREOL, University of Central Florida, PO Box 162700, Orlando, FL 32816-2700, USA*

Received 9 July 1999

**Abstract**

The response of an antenna-coupled microbolometer fabricated on a Si wafer coated on both sides with thin films of $SiO_2$ was measured for two types of illumination: through the substrate and from the air side. The measurement was performed in the spectral range from 9.22 to 10.84 μm. Both cases are modeled by using the transmission, reflection, and absorption properties of the three-layer wafer. The spectral characteristics of the $SiO_2$ thin film play a major role in the response of the detector. The responses of the sensor to the parallel and perpendicular polarizations are modeled by using two main contributions: the heating by absorption in the $SiO_2$ layer and the coupling of incident flux on the bolometer. Fitting this model to the experimental data allows us to conclude that the antenna response is the result of the incident flux coming from the substrate side. When the device is illuminated from the air side, the antenna signal results from the flux reflected at the film/substrate interface. The efficiencies of the contributions to the antenna signal coming from the substrate or from the air side have been obtained from the data fitted with the model. The substrate-side contribution is 50 times larger than the air-side contribution, confirming the theory of lithographic antenna on a dielectric substrate. 

*Keywords:* Microbolometer; Integrated infrared antenna; Infrared detector; Layered substrate

## 1. Introduction

Antenna-coupled metal-oxide-metal diodes and microbolometers have been demonstrated in the infrared at wavelengths near 10 μm [1–4]. In a typical configuration, these devices are illuminated through the substrate to provide a better coupling efficiency to the antenna structure. However, from a practical point of view, the substrate-side illumination configuration precludes monolithic integration of the de-

[*] Corresponding author. Tel.: +1-407-823-2979; fax: +1-407-823-6880.

*E-mail addresses:* j.alda@fis.ucm.es (J. Alda), cfumeaux@mail.creol.ucf.edu (C. Fumeaux).

[1] Permanent address: Optics Department, School of Optics, University Complutense of Madrid, Avda. Arcos de Jalón s/n, 28037 Madrid, Spain.

[2] Cornell Nanofabrication Facility, Knight Laboratory, Cornell University, Ithaca, NY 14853-5403, USA.

1350-4495/00/$ - see front matter 
PII: S1350-4495(99)00036-5

vice with existing readout and multiplexer electronics.

The rule of thumb to establish the best option for illumination uses the relative efficiency of a microstrip antenna located in the interface between two media having different electrical permittivities [5 6]. The ratio $\Gamma$ of the power $\Phi$ radiated by the antenna into the two media is

$$\Gamma = \frac{\Phi_1}{\Phi_2} \approx \left( \frac{\epsilon_1}{\epsilon_2} \right)^{3/2} \quad (1)$$

where $\epsilon_1$ and $\epsilon_2$ are the dielectric constant of the two media. By reciprocity, the ratio $\Gamma$ describes the relative coupling efficiency of an antenna at the interface. Given that $\epsilon_{Si} = 11$ and the small thickness of the $SiO_2$ layer, this means that the coupling of the energy to the antenna will be 40 times more efficient for the light incident from the substrate than from the air side at infrared frequencies.

Eq. (1) would seem to indicate that substrate-side illumination is the only viable alternative. However, in our experiments and in some other previous work [2], we observed a strong antenna response when the device was illuminated from the air side, even at visible frequencies [7]. The values of response are of the same order as those obtained by illuminating through the substrate. These observations called into question the validity of Eq. (1) and prompted us to pursue a clearer picture of the illumination mechanism of the device. To accomplish this, we measured the spectral dependence of the responsivity for both illumination configurations and related it to the spectral characteristics of the wafer structure.

In Section 2 we present the device, its characteristic parameters, and the experimental setup used to perform the measurements. The theoretical model used to analyze the data is presented in Section 3, where the transmission, reflection, and absorption of the different layers of the structure are evaluated. The results obtained from the experiment are fitted with the model and analyzed in Section 4. The conclusions of this paper are summarized in Section 5.

## 2. Detector and experimental setup

Fig. 1 shows an electron micrograph of the device measured in this work. It is a Nb-microbolometer coupled to an aluminum dipole antenna. The response of this type of device shows a strong polarization dependence with a maximum signal when the electric field is parallel to the dipole, as expected from antenna theory. Antennas are used to enhance the power collection efficiency of detectors that are much smaller than the incident wavelength.

The devices are fabricated onto a high-resistivity Si wafer ($\rho > 3000\ \Omega$ cm) of 380-μm thickness. The wafer is polished on both sides and coated with a thermally grown 1.5-μm $SiO_2$ insulating layer. The metallic structures, with a width on the order of 200 nm, are defined with a direct-write electron-beam lithography tool (Cambridge, EMBF 10.5).

The antenna was illuminated with a tunable $CO_2$ laser capable of oscillating in a $TEM_{00}$ at several transitions ranging from 9.22 to 10.84 μm in wavelength. The output power of the laser was monitored continuously to provide a reference signal for normalization. The beam was modulated with a mechanical chopper synchronized to a lock-in amplifier that read the signal from the device. The polarization direction of the beam was controlled by means of a $\lambda/2$ plate. The beam was collimated and focused using aspheric $F/1$ optics to a spot size of around 15 μm in radius. The microbolometer was mounted on a three-dimensional micropositioning stage that allowed us to locate the detector in the volume of maximum irradiance of the focused spot. When the wavelength of the laser was changed it was necessary to move the device slightly along the optical axis to compensate for the focal shift produced by the change in wavelength. At each wavelength two measurements were performed, one for each orthogonal polarization direction (parallel and perpendicular to the antenna structure). The measurements were done for the air-incidence and substrate-incidence configurations at normal incidence.

## 3. Theoretical model

The light that interacts with the microbolometer detector and its antenna also interacts with the underlying structure on which the device is fabricated. To characterize and determine the role of the wafer materials, we have measured the reflection and transmission spectra of the wafers supporting the device (see Fig. 2). This measurement was made using a

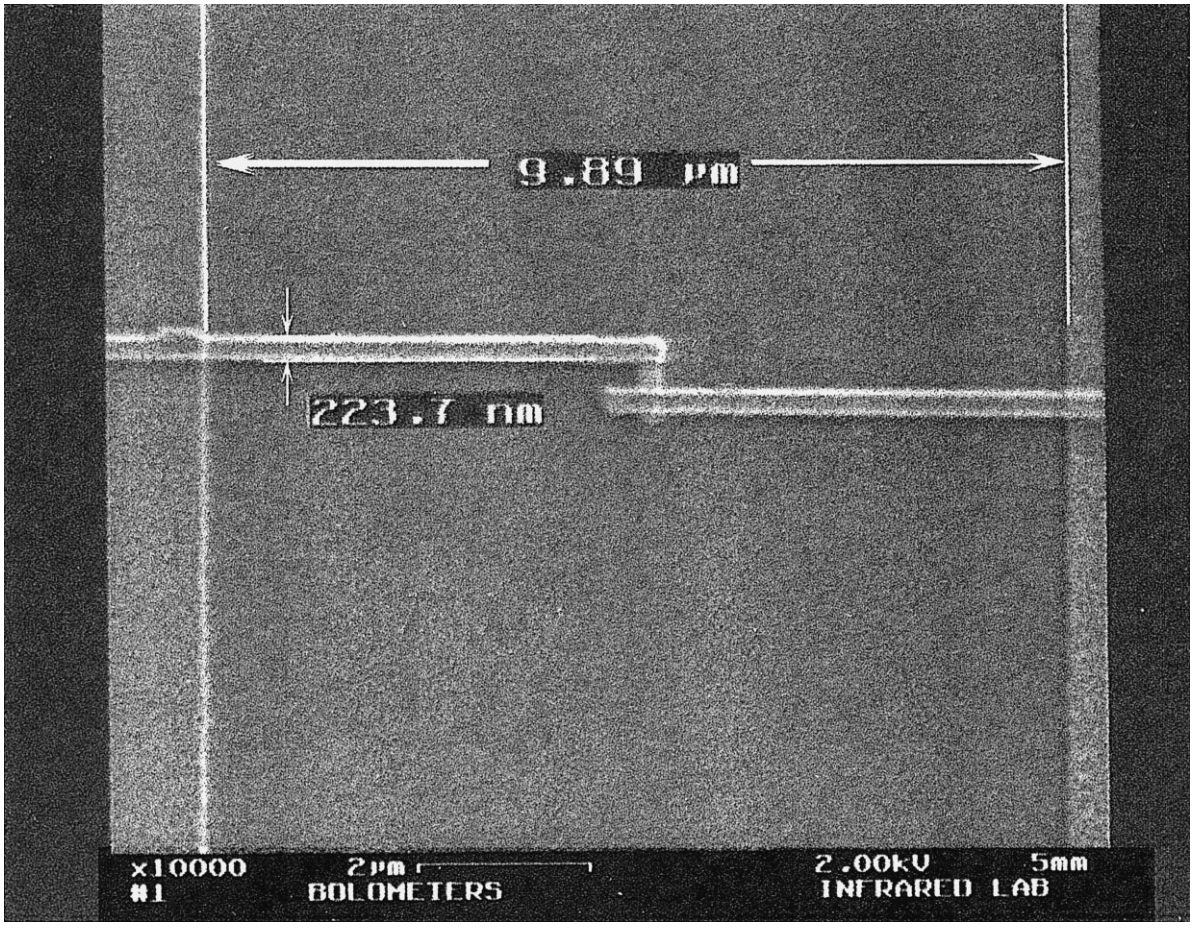


Fig.1. Electron microscope photograph of the microbolometer used in this paper.

Fourier-transform infrared spectrometer, FTIR (Perkin-Elmer 1710). The wafer structure has been modeled as follows. The $SiO_2$ layers are considered as thin films deposited on both sides of a thick Si substrate. The thickness of the $SiO_2$ layer, measured by ellipsometry, is 1.5 μm and the Si wafer thickness is specified at around 380 μm. For these $SiO_2$ thin films, it is necessary to take into account the multiple-interference mechanisms that modify the transmission, reflection, and absorption of the structure depending also on the order of the arrangement of the layers (Air/$SiO_2$/Si or Si/$SiO_2$/Air) [8]. On the contrary, interference effects are neglected for the thick Si substrate. The experimental setup used to measure the detector response provides a very tightly focused beam whose Rayleigh range is in the order of 100 μm. In this case the contributions of multiple reflections in Si are negligible because of the large dilution of the irradiance for the successive reflected contributions. A spectral response of this layered structure is calculated using measured index-of-refraction values for Si and $SiO_2$ from the literature [9–11]. The results obtained from this model are compared to the measurements from the spectrometer. The complex index of refraction for $SiO_2$ is adjusted from the literature starting values to accomplish a fit of the measured data. We choose to adjust the optical constants of the $SiO_2$ layer because they show the strongest influence on the spectral properties of the structure in the wavelength range of interest. In addition, the optical properties of this layer will be influenced by the purity and the micro-

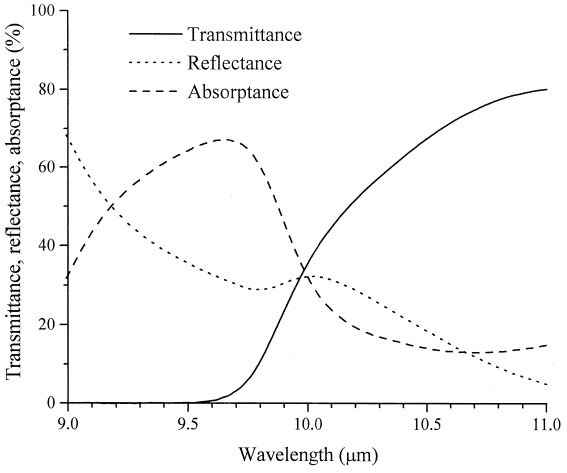


Fig. 2. Measured spectra for the transmission and reflection of the wafer obtained from an infrared Fourier-transform spectrometer. The absorption has been calculated from the values of the transmission and reflection.

scopic arrangement of the material. The calculated index of refraction of the $SiO_2$ (real and imaginary parts) is shown in Fig. 3 with the values obtained from the literature [10]. The fitted values for the index of refraction are used to model the expected reflection, transmission, and absorption of each material interface and layer involved in the design.

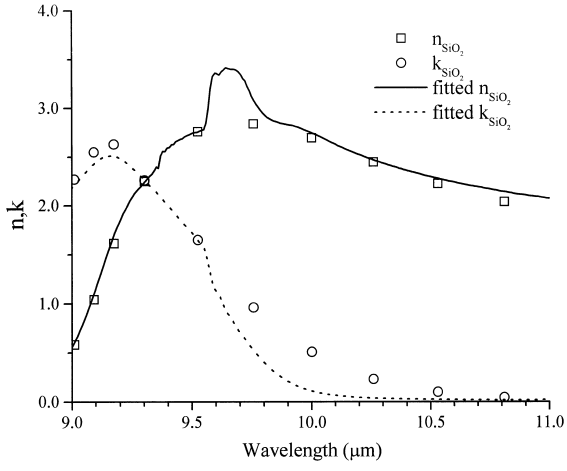


Fig. 3. Calculated index of refraction of the $SiO_2$ that is obtained to fit the spectral characteristic of the wafer. The starting values of the fitting are those provided by Ref. [10], and are indicated by squares and circles.

The change in temperature of the bolometer is produced by two basic mechanisms: from absorption of flux in the $SiO_2$ layer adjacent to the bolometer and from direct heating of the bolometer structure. This last contribution is responsible for the polarization-dependent response of the device, because it contains the signal caused by dissipation in the bolometer of current waves excited in the antenna arms. The absorption of the $SiO_2$ layer is primarily responsible for the heating of the materials near the

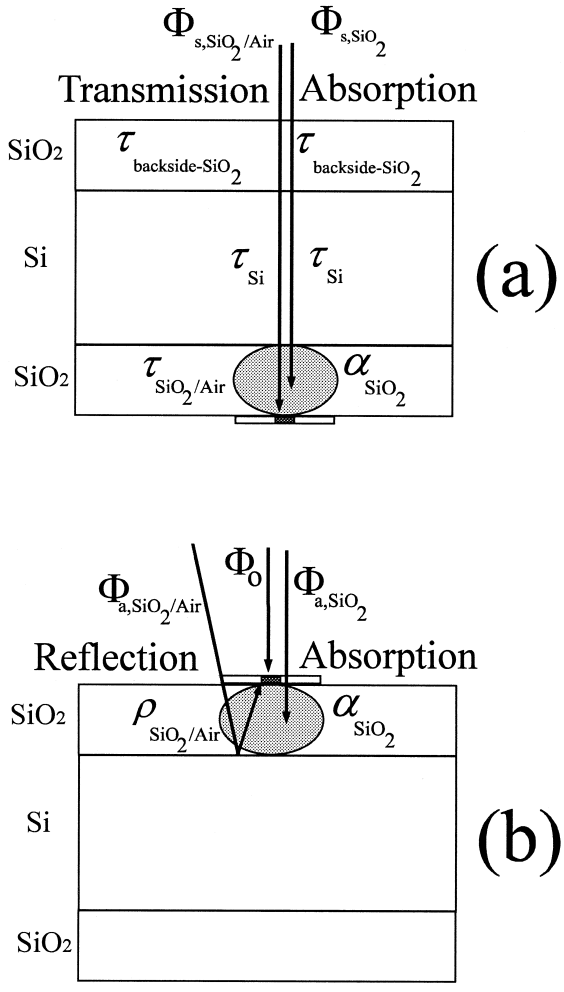


Fig. 4. Schematic of the different contributions to the signal of the detectors, (a) incidence from the substrate, (b) incidence from the air. The actual values of the thickness of the films and susbstrate are 1.5 μm for the $SiO_2$ layers, and 380 μm for the Si. The reflection contribution is not depicted in normal incidence for clarity.

bolometer. The part of the response caused by the energy coupled to the dipole antenna is proportional to the incident flux on the plane of the bolometer. This relative strength of both flux terms can be calculated in terms of the transmission and reflection of the layers that compose the structure (see Fig. 4), using the fitted index values obtained from the FTIR data. If we assume that the incident flux on the wafer is constant for the spectral range of interest, then the spectral characteristics of the transmittance, reflectance, and absorbance will produce a wavelength dependence of the absorbed and transmitted flux, and therefore a sensor response that will depend on the wavelength of the incident light.

### 3.1. Substrate-side illumination

For incidence from the substrate side, the different contributions to the response of the detector are as follows. The response of the bolometer for the polarization state perpendicular to the dipole, $V_{\perp,s}$, can be considered a thermal response [2,3] and is mainly caused by the absorption of the $SiO_2$ layer. The subscripts indicate the type of polarization ($\perp$, perpendicular to the dipole antenna; $\parallel$, parallel to the dipole antenna) and the illumination direction (s denotes incidence from the substrate side and a denotes incidence from the air side). To evaluate the absorbed flux in the $SiO_2$ it is first necessary to calculate the flux that reaches the $SiO_2$ layer adjacent to the antenna. This flux has been transmitted through the backside $SiO_2$ layer as well as the Si bulk substrate. Then, the absorbed flux in the $SiO_2$ layer closest to the antenna is calculated (see Fig. 4a) as,

$$\Phi_{s,SiO_2} = \left(\alpha_{s,SiO_2} \times \tau_{Si} \times \tau_{backside-SiO_2}\right)\Phi_o, \qquad (2)$$

where $\Phi_o$ represents the incident flux on the wafer, $\tau_{backside\text{-}SiO_2}$ is the transmittance of the backside $SiO_2$ layer, $\tau_{Si}$ is the transmittance of the Si thick layer, and $\alpha_{s,SiO_2}$ is the absorption of the $SiO_2$ layer adjacent to the bolometer. Multiple reflection effects have been taken into account in both thin layers.

In addition to the absorbed flux contribution, is a heating of the bolometer structure that is proportional to the incident flux onto the bolometer and caused by the absorption of the structure of the bolometer itself and its metallic connections. The incident flux at the $SiO_2/Air$ interface where the bolometer is located is calculated taking into account the Si transmission and the multiple reflections in both $SiO_2$ layers. In the layer adjacent to the antenna, only those beams propagating from the $Si/SiO_2$ interfaces toward the $SiO_2/Air$ interface are added. This calculation can be written as

$$\Phi_{s,SiO_2/Air} = \left(\tau_{s,SiO_2/Air} \times \tau_{Si} \times \tau_{backside-SiO_2}\right)\Phi_o, \qquad (3)$$

where $\tau_{s,\,SiO_2/Air}$ represents the contribution of those beams propagating from the $Si/SiO_2$ interface to the $SiO_2/Air$ interface in the $SiO_2$ layer adjacent to the detector. These flux terms, $\Phi_{s,SiO_2}$ and $\Phi_{s,SiO_2/Air}$ are plotted in Fig. 5 as a function of wavelength.

The same two fluxes that cause the perpendicular response, $\Phi_{s,SiO_2}$ and $\Phi_{s,SiO_2/Air}$ will also be responsible for the response obtained when the polarization is parallel to the dipole antenna, $V_{\parallel,s}$. In this case, the contribution of the antenna-coupled radiation to the parallel response will be proportional to the flux incident onto the bolometer, $\Phi_{s,SiO_2/Air}$. By using the

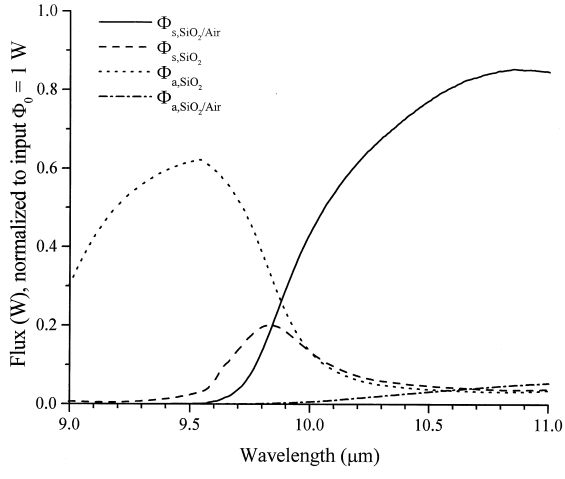


Fig. 5. Plot of the absorbed flux in the $SiO_2$ layer adjacent to the bolometer for the substrate and air incidence configurations, $\Phi_{s,SiO_2}$ and $\Phi_{a,SiO_2}$, respectively. We also plot the incident flux on the bolometer coming from the $SiO_2$ side of the $SiO_2/Air$ interface, for the substrate and air incidence illuminations, $\Phi_{s,SiO_2/Air}$ and $\Phi_{a,SiO_2/Air}$, respectively. We are assuming that the incident flux is constant along the spectral range, $\Phi_o = 1$ W.

calculated absorbed and incident fluxes, Eqs. (2) and (3), it is possible to write the response of the bolometer for the two polarization states as

$$V_{\perp,s} = \eta_{\perp,s,SiO_2}\Phi_{s,SiO_2} + \eta_{\perp,s,SiO_2/Air}\Phi_{s,SiO_2/Air} \quad (4)$$

and

$$V_{\parallel,s} = \eta_{\parallel,s,SiO_2}\Phi_{s,SiO_2} + \eta_{\parallel,s,SiO_2/Air}\Phi_{s,SiO_2/Air}, \quad (5)$$

where the coefficients $\eta_{\perp,s,SiO_2}$, $\eta_{\perp,s,SiO_2/Air}$, $\eta_{\parallel,s,SiO_2}$, and $\eta_{\parallel,s,SiO_2/Air}$ are the conversion efficiencies of the corresponding mechanisms in producing a response. In the case of perpendicular polarization, $\eta_{\perp,s,SiO_2/Air}$, is related to the thermal absorption of the bolometer structure. For parallel polarization, $\eta_{\parallel,s,SiO_2/Air}$, will account for the antenna-coupled contribution. The antenna response $\Delta V_s$ is taken as the difference between the parallel and perpendicular responses, $\Delta V_s = V_{\parallel,s} - V_{\perp,s}$.

### 3.2. Air-side illumination

When radiation is incident on the antenna from the air side, the contributing mechanisms are of the same type as for substrate-side illumination (see Fig. 4b). The response $V_{\perp,a}$ (the subscript a indicates air incidence) is produced by the absorbed flux in the front $SiO_2$ layer, and from the heating of the structure of the device caused by the flux incident onto the plane of the device. The absorbed flux is now calculated as

$$\Phi_{a,SiO_2} = \alpha_{a,SiO_2}\Phi_o, \quad (6)$$

where $\alpha_{a,SiO_2}$ is the absorption coefficient of the $SiO_2$ layer adjacent to the bolometer (taking into account the multiple reflections). The flux incident on the bolometer comes from the air side, being proportional to $\Phi_o$, and also from the $SiO_2$ side. This last incident flux can be written as

$$\Phi_{a,SiO_2/Air} = \rho_{a,SiO_2/Air}\Phi_o \quad (7)$$

where $\rho_{a,SiO_2/Air}$ accounts for the light reflected at the $SiO_2$/Si interface and arriving to the $SiO_2$/Air interface, taking into account the multiple reflections in the $SiO_2$ thin film. The possible contribution coming from the reflection of the flux in the substrate side $SiO_2$ structure is neglected because in our experimental conditions the beam is tightly focused. In Fig. 5, we plotted the spectral dependence of $\Phi_{a,SiO_2}$ and $\Phi_{a,SiO_2/Air}$.

These two contributions, caused by the fluxes $\Phi_o$ and $\Phi_{a,SiO_2/Air}$, appear together in the air-side illumination case only. For the substrate-side illumination case, no structure reflects radiation back to the detector. The coupling efficiency of the radiation to the antenna structure is different for the reflected flux, $\Phi_{a,SiO_2/Air}$, and for the flux incident directly, $\Phi_o$. The ratio is theoretically given by Eq. (1) and will be introduced in our calculation as $\Gamma$.

When the electric field is polarized parallel to the dipole antenna, the power coupled by the dipole will not contribute to the heating mechanism in the interior of the $SiO_2$ layer. The relative efficiencies of the thermal and antenna mechanisms to change the temperature of the bolometer and therefore to provide a measurable signal are different. For certain wavelengths, a parallel signal lower than the cross-polarization (perpendicular) signal was observed. This apparently anomalous behavior can be interpreted as follows. The incident flux, $\Phi_o$, must be shared by the absorption in the $SiO_2$ and by the antenna-coupling mechanism. Therefore, when the antenna is allowed to couple energy (because the electric field is properly aligned), then the absorption mechanism has less power available.

We thus have the following expressions for the perpendicular and parallel responses:

$$V_{\perp,a} = \eta_{\perp,a,SiO_2}\Phi_{a,SiO_2} + \eta_{\perp,a,SiO_2/Air}\left(\Phi_o + \Phi_{a,SiO_2/Air}\right) \quad (8)$$

and

$$\begin{aligned} V_{\parallel,a} &= \eta_{\parallel,a,SiO_2}\Phi_{a,SiO_2} + \eta^{bol}_{\parallel,a,SiO_2/Air}\left(\Phi_o + \Phi_{a,SiO_2/Air}\right) + \eta^{ant}_{\parallel,a,SiO_2/Air}\left(\Phi_o + \Gamma\Phi_{a,SiO_2/Air}\right) \\ &\approx \eta_{\parallel,a,SiO_2}\Phi_{a,SiO_2} + \eta_{\parallel,a,SiO_2/Air}\left(\Phi_o + \Gamma\Phi_{a,SiO_2/Air}\right), \end{aligned} \quad (9)$$

where the coefficients $\eta_{\perp,a,SiO_2}$ and $\eta_{\parallel,a,SiO_2}$ are the conversion efficiencies of the absorption in the $SiO_2$ layer. The coefficient $\eta_{\perp,a,SiO_2/Air}$ represents the efficiency to produce a response from the heating of the structure of the bolometer caused by the incident radiation coming from both sides of the Air/$SiO_2$ interface. Correspondingly, $\eta^{bol}_{\parallel,a,SiO_2/Air}$ and $\eta^{ant}_{\parallel,a,SiO_2/Air}$ describe the efficiency of the thermal and antenna coupling in the bolometer structure for parallel polarization. Eq. (9) is approximated to al-

low a comparison of the coefficients for the parallel and perpendicular responses. This approximation considers that the thermal coupling of the flux in the bolometer structure is negligible for the parallel polarization when the flux is coupled to the antenna structure, i.e., $\eta^{\mathrm{bol}}_{\parallel,\mathrm{a},\mathrm{SiO_2/Air}} \ll \Gamma\eta^{\mathrm{ant}}_{\parallel,\mathrm{a},\mathrm{SiO_2/Air}}$, and therefore $\eta^{\mathrm{ant}}_{\parallel,\mathrm{a},\mathrm{SiO_2/Air}} \approx \eta_{\parallel,\mathrm{a},\mathrm{SiO_2/Air}}$. For the parallel polarization it has been necessary to include the $\Gamma$ factor from Eq. (1) to weight the contribution of the two beams incident onto the antenna, one coming from the air and the other from the $SiO_2$. If the incoming flux, $\Phi_o$, is assumed to be constant along the spectral range of interest, then the effect of the air-side direct incident flux can be associated with a global positive offset for the total spectral range. This term does not appear explicitly in the case of substrate incidence because there is no contribution of flux incident from the air side. Therefore, because in the substrate-side illumination the flux is coming from the substrate, $\Gamma$ is included in the value of $\tau_{\parallel,\mathrm{s}}$. This factor $\Gamma$ is assumed to be constant for the spectral range of interest because the change in the value of the refraction index of the Si is negligible.

## 4. Experimental results and analysis

The spectral response of a bolometer with an antenna length of about 10 μm has been measured to obtain the values of the $V_{\perp,\mathrm{s}}$, $V_{\parallel,\mathrm{s}}$, $V_{\perp,\mathrm{a}}$, and $V_{\parallel,\mathrm{a}}$. These data have been fitted with the model expressed in Eqs. (4), (5), (8), and (9) normalized to a flux of $\Phi_o = 1$ W, independent of the wavelength.

The efficiencies related with the absorbed flux ($\eta_{\perp,\mathrm{s},\mathrm{SiO_2}}$, $\eta_{\parallel,\mathrm{s},\mathrm{SiO_2}}$, $\eta_{\perp,\mathrm{a},\mathrm{SiO_2}}$, and $\eta_{\parallel,\mathrm{a},\mathrm{SiO_2}}$), the incident flux ($\eta_{\perp,\mathrm{s},\mathrm{SiO_2/Air}}$, $\eta_{\parallel,\mathrm{s},\mathrm{SiO_2/Air}}$, $\eta_{\perp,\mathrm{a},\mathrm{SiO_2/Air}}$, and $\eta_{\parallel,\mathrm{a},\mathrm{SiO_2/Air}}$), and the antenna-coupling efficiency ratio ($\Gamma$) for the best fitting of the experimental data are shown in Table 1. The fitting procedure used a minimum-squared-difference algorithm to find the values of the parameters. The graphical representation of the fitting of the model with the experimental data is shown in Fig. 6 for the two cases of illumination geometry. In this figure, we have represented the response for the perpendicular and parallel polarizations of the incident radiation, $V_\perp$ and $V_\parallel$, and also their difference, $\Delta V = V_\parallel - V_\perp$. The difference $\Delta V$ corresponds primarily to the antenna-coupling effect [3].

Table 1
Coefficients of the fitting of the model with the experimental data. All the values are in μV/W, except $\Gamma$ that is dimensionless

| Substrate-side illumination | | Air-side illumination | |
|---|---|---|---|
| $\eta_{\perp,\mathrm{s},\mathrm{SiO_2}}$ | 2195 | $\eta_{\perp,\mathrm{a},\mathrm{SiO_2}}$ | 3142 |
| $\eta_{\parallel,\mathrm{s},\mathrm{SiO_2}}$ | 2097 | $\eta_{\parallel,\mathrm{a},\mathrm{SiO_2}}$ | 2495 |
| $\eta_{\perp,\mathrm{s},\mathrm{SiO_2SiO/Air}}$ | 535 | $\eta_{\perp,\mathrm{a},\mathrm{SiO_2/Air}}$ | 434 |
| $\eta_{\parallel,\mathrm{s},\mathrm{SiO_2/Air}}$ | 1468 | $\eta_{\parallel,\mathrm{a},\mathrm{SiO_2/Air}}$ | 21 |
| | | $\Gamma$ | 50 |
| | | $\Gamma\eta_{\parallel,\mathrm{a},\mathrm{SiO_2/Air}}$ | 1021 |

An analysis of the efficiencies of the absorbed flux shows that $\eta_{\parallel,\mathrm{s},\mathrm{SiO_2}} < \eta_{\perp,\mathrm{s},\mathrm{SiO_2}}$ and $\eta_{\parallel,\mathrm{a},\mathrm{SiO_2}} < \eta_{\perp,\mathrm{a},\mathrm{SiO_2}}$.The decrease of the contribution of the absorption in the $SiO_2$ when the orientation of the polarization is along the dipole antenna can be explained by assuming that the same amount of incident flux has to be shared by two competing mechanisms with relative importance of the same order: the absorption and the antenna coupling. For the cross-polarization state, the competition is between the absorption inside the $SiO_2$ layer and the thermal absorption of the bolometer structure, with the latter being less important than the absorption in the $SiO_2$. In addition, although the absorption mechanism is the same, the difference between the parallel and perpendicular polarization efficiencies is also caused by the way the multiple reflections work. In the case of parallel polarization, every time the light reaches the $SiO_2$/Air interface, it can be coupled to the antenna, leaving less flux available for the absorption inside the $SiO_2$ layer in the successive bounces. This effect diminishes the conversion efficiency of the absorbed flux into signal for the parallel-polarization case.

When comparing the coefficients that multiply the flux incident on the antenna plane coming from the $SiO_2$ layer, we find that $\eta_{\parallel,\mathrm{s},\mathrm{SiO_2/Air}} > \eta_{\perp,\mathrm{s},\mathrm{SiO_2/Air}}$ and $\Gamma\eta_{\parallel,\mathrm{a},\mathrm{SiO_2/Air}} > \eta_{\perp,\mathrm{a},\mathrm{SiO_2/Air}}$. In this case, the increase of the parallel multiplicative efficiencies compared to the corresponding perpendicular ones is caused by the flux coupled to the antenna structure. From the data of the fitting (see Table 1) we can see that the ratio between the parallel and perpendicular factors is about the same for the two types of incidence (2.7 for the substrate-side incidence and 2.4 for the air-side incidence).

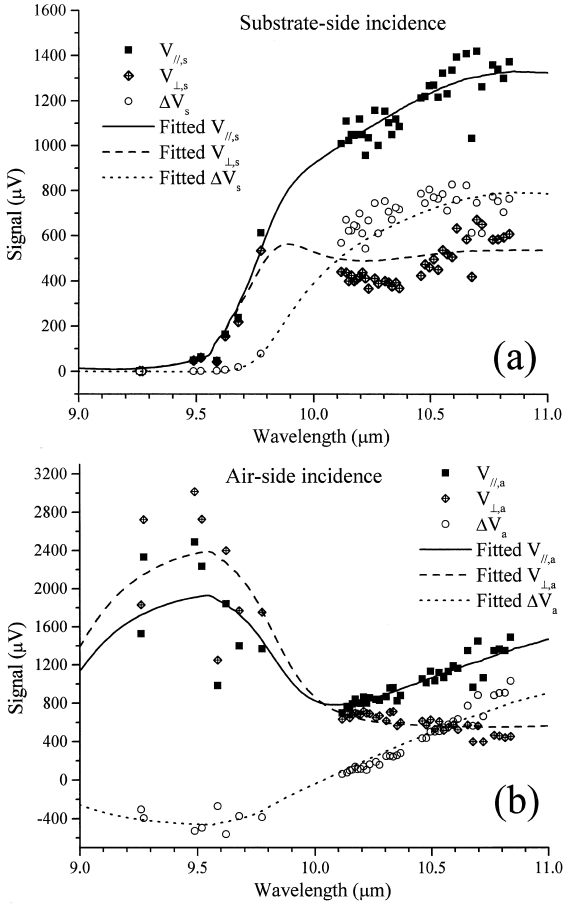


Fig. 6. Plot of the values of the response of the devices for the parallel and perpendicular orientations of the electric field with respect to the dipole antenna. The difference between the parallel and the perpendicular polarization responses is associated with the antenna response and is also represented in the plot. The results of the fitting of the model with the experimental data are also plotted for the parallel polarization, the perpendicular polarization and their difference. Fig. 6(a) is for the substrate-side illumination case, and Fig. 6(b) is for the air-side incidence.

It is obvious from Fig. 6 that the antenna response, $\Delta V$, is strongly dependent on the spectral characteristics of the $SiO_2$ layer. This was expected and observed previously by other authors [2]. For the substrate-side incidence, the two $SiO_2$ layers and the Si substrate transmissivities influence the final result. In this case, it is clear that when no light reaches the antenna structure it is not possible to obtain any useful signal. For the air-side incidence case, the main role is played by the first $SiO_2$ layer. Its spectral reflectivity and absorption determine the spectral response of the devices. As demonstrated with the model, the back $SiO_2$ layer does not play any role in our fast-focusing experimental conditions. This observation is justified because the Si substrate is thick enough to prevent appearance of interference effects for the focused laser beams used in the experiment. However, if more collimated light is used and the light can be reflected from the backside layer, then the whole wafer structure should be taken into account to calculate the total flux incident onto the antenna coming from the substrate side.

The observed change in the direction of the maximum polarization orientation observed for air-side incidence is also explained by the model. The decreased absorption for the parallel response allows the existence of larger response for the perpendicular polarization direction than for the parallel in the spectral regions where the absorption-derived signal is dominant.

An important conclusion that can be reached from the data is that the amount of flux coupled to the antenna when light is incident from the air side directly (without reflection in any underlying structure) is significantly lower than from the substrate side. The antenna response almost disappears in the spectral regions for which the $SiO_2$ layer is nearly opaque. In our model, the relative efficiency of the coupling of the energy to the antenna structure is given by $\Gamma$. The results of the fitting provide a value of $\Gamma$ of 50 for the measured bolometer that is in good agreement with the theoretical value of 40 (see Eq. (1)) and explains the behavior of the antenna. It should be noted that this ratio of coupling, $\Gamma$, is not interpreted as the ratio between the antenna responses for the air-side incidence and the substrate-side incidence, $\Delta V_a/\Delta V_s$. For example, at $\lambda = 10.6$ μm, we obtained a ratio of $\Delta V_a/\Delta V_s = 0.84$. This allows a practical operation of the device for the air-side incidence configuration.

## 5. Conclusions

The response of antenna-coupled microbolometers has been modeled in terms of the spectral characteristics of the layered wafer structure composed of two $SiO_2$ thin films that enclose a thick Si substrate. The complex index of refraction of the $SiO_2$ layer of the

wafer is evaluated using measured values of spectral reflectance and transmittance, and a slight adjustment of the values of the index of refraction referred to in the literature is obtained.

The contributions of the different mechanisms to the total response are accounted for with two terms. One of them is the absorption of the $SiO_2$ layer whose thermal heating provides most of the polarization-independent signal. The second term is caused by the flux incident onto the microbolometer plane. This flux is related to the transmission of the whole wafer when illuminating from the substrate, and has two components for the case of illumination from the air. In this last case, the light can reach the bolometer coming from the incident beam directly, and also from the reflection at the $SiO_2/Si$ interface. The results presented in this paper show that the antenna-coupled bolometers can be illuminated from the air and a polarization-dependent response is obtained. However, for the air incidence, the relevant mechanism in the antenna response is the coupling of electromagnetic energy reaching the antenna from the inside of the $SiO_2$ layer. This fact is in good agreement with the expected efficiency of the detection of an antenna on a substrate in terms of the ratio between the index of refraction on both sides of the antenna.

The irrelevance of the back surface characteristics for the air-side-incidence case allows a proper integration of the detectors with auxiliary electronics. However, special attention must be given to the material characteristics and thickness of the insulating layer (made of $SiO_2$ for our devices). The spectral dependence of the complex index of refraction of the material used and the role of the multiple reflections inside the layer modify the spectral response of the device. Finally, as expected from the theoretical results, the amount of power coupled to the antenna from the air-side direct incident flux is not large enough to produce a useful response of the device. For the air-side illumination, the radiation reflected in the substrate produces a much larger contribution. However, the ratio between the antenna responses for the air-side illumination and the substrate-side illumination is $\Delta V_a/\Delta V_s = 0.84$ at $\lambda = 10.6$ μm, that makes the air-side incidence practical.

Summarizing, illumination of the antenna-coupled microbolometers from the air side is possible and primarily depends on the characteristics of the thin-film insulating layer on which the device is fabricated. Its spectral characteristics primarily depend on the thickness and the values of the complex index of refraction of the material used. An appropriate choice of these parameters would allow tailoring of the spectral response for a given application.

## Acknowledgements

We are grateful to Irina Puscasu who made the infrared Fourier-transform spectra of the substrate. J. Alda is supported by a scholarship (PR1997-0252) from the Ministerio de Educación y Cultura of Spain, and by a grant from the School of Optics of the University of Central Florida. We also acknowledge the support of the US Ballistic Missile Defense Organization (BMDO) and Lockheed-Martin Corporation.

## References

[1] I. Wilke, W. Herrmann, F.K. Kneubühl, Integrated nanostrip dipole antennas for coherent 30 THz infrared radiation, Appl. Phys. B 58 (1994) 87–95.
[2] I. Wilke, Y. Oppliger, W. Herrmann, F.K. Kneubühl, Nanometer thin-film Ni–NiO–Ni diodes for 30 THz radiation, Appl. Phys. A 58 (1994) 329–341.
[3] C. Fumeaux, W. Herrmann, F.K. Kneubühl, H. Rothuizen, Nanometer thin-film Ni–NiO–Ni diodes for detection and mixing of 30 THz radiation, Infrared Phys. Technol. 39 (1998) 123–183.
[4] E.N. Grossman, J.E. Sauvageau, D.G. McDonald, Lithographic spiral antennas at short wavelengths, Appl. Phys. Lett. 59 (1991) 3225–3227.
[5] C.R. Brewitt-Taylor, D.J. Gunton, H.D. Rees, Planar antennas on a dielectric surface, Electron. Lett. 17 (1981) 729–730.
[6] D.B. Rutledge, M.S. Muha, Imaging antenna arrays, IEEE Trans. Antennas Propagation AP-30 (1982) 535–540.
[7] C. Fumeaux, J. Alda, G.D. Boreman, Lithographic antennas at visible frequencies, Opt. Lett. 24 (1999) 1629–1631.
[8] R.M.A. Azzam, N.M. Bashara, Ellipsometry and Polarized Light, North-Holland, Amsterdam, 1987, Chapter 4.
[9] D.F. Edwards, Silicon (Si), in: E.D. Palik (Ed.), Handbook of Optical Constants of Solids, Academic Press, New York, 1985, pp. 547–569.
[10] H.R. Philipp, Silicon dioxide ($SiO_2$) (Glass), in: E.D. Palik (Ed.), Handbook of Optical Constants of Solids, Academic Press, New York, 1985, pp. 749–763.
[11] H.R. Philipp, The infrared optical properties of $SiO_2$ and $SiO_2$ layers on silicon, J. Appl. Phys. 50 (1979) 1053–1057.